

**SYNTHESIS OF Cs-POLLUCITE NANOZEOLITE
AND CATALYTIC STUDY IN BASE-
CATALYZED BENZALDEHYDE
CONDENSATION REACTIONS**

ALEID, GHADAH MOHAMMAD S

UNIVERSITI SAINS MALAYSIA

2020

**SYNTHESIS OF Cs-POLLUCITE NANOZEOLITE
AND CATALYTIC STUDY IN BASE-
CATALYZED BENZALDEHYDE
CONDENSATION REACTIONS**

by

ALEID, GHADAH MOHAMMAD S

**Thesis submitted in fulfilment of the requirement
for the degree of
Doctor of Philosophy**

May 2020

ACKNOWLEDGEMENT

I would like to express my sincere gratitude and appreciation to my supervisor Assoc. Prof. Dr. Ng Eng Poh for his expert guidance, valuable assistance, motivation and immense knowledge towards the realization of this study. His enormous knowledge has helped me a lot throughout my research work. I would also like to acknowledge Universiti Sains Malaysia (USM), Université de Caen (France), Université de Haute-Alsace (France), Université de Strasbourg (France) and Universiti of Malaya for the availability of the needed facilities which enable the success of my project. My appreciation also goes to RUI (1001/PKIMIA/8011012) and FRGS (203/PKIMIA/6711642) grants for the financial support. Also, I am grateful to the University of Hail, Saudi Arabia (UOH) who provided scholarship and allowed me to do study in USM. A very special thanks go to all staff of the School of Chemical Sciences, USM that have contributed enormously throughout my research. My heartfelt gratitude to my lab mates Mrs. Tamara, Ms. Nurhidayahni, Ms. Cythia, Dr. Haruna and Mr. Ismail for their advice, support, guidance and encouragement during my PhD study in Universiti Sains Malaysia. Last but not least, my deepest appreciation dedicates to my parents, husband and kids for their love, support, patience and faith in me. All my accomplishments will not be possible without them in my life.

TABLE OF CONTENTS

ACKNOWLEDGEMENT	ii
TABLE OF CONTENTS	iii
LIST OF TABLES	viii
LIST OF FIGURES	ix
LIST OF SYMBOLS AND NOMENCLATURES	xiv
ABSTRAK	xvi
ABSTRACT	xviii
CHAPTER 1 INTRODUCTION	1
1.1 General introduction.....	1
1.2 Research objectives	7
1.3 Overview of the thesis.....	7
CHAPTER 2 LITERATURE REVIEW	10
2.1 Introduction	10
2.2. Discovery and history of zeolites	10
2.3 Structure of zeolites.....	12
2.4 Effect of synthesis parameters on the formation of zeolites	14
2.4.1 Alkalinity	14
2.4.2 Effect of temperature	15
2.4.3 Effect of time	15
2.4.4 Effect of mineralizing agents (OH ⁻)	16
2.4.5 Effect of the Si/Al ratio	16
2.4.6 Effects of water content	17
2.5 Nanosized zeolites.....	17
2.6 Zeolite synthesis and formation	19
2.7 Cesium aluminosilicate zeolites	22

2.8	Applications of zeolites.....	23
2.8.1	Zeolites in adsorption and separation	23
2.8.2	Zeolites in ion exchange	24
2.8.3	Zeolites in catalysis	25
2.8.3(a)	Aldol condensation of benzaldehyde with acetic anhydride (Perkin condensation).....	27
2.8.3(b)	Aldol condensation of benzaldehyde with acetophenone (Claisen - Schmidt condensation).....	29
2.9	Hierarchization in zeolites.....	31
2.10	Templating methods.....	33
2.11	Heating method	36
2.11.1	Microwave heating.....	36
2.11.2	Non-microwave instant heating	37
CHAPTER 3 MATERIALS AND EXPERIMENTAL METHODS		39
3.1	Introduction.....	39
3.2	Chemicals.....	39
3.3	Synthesis of Cs-pollucite zeolite nanocrystals under different crystallization conditions	40
3.4	Synthesis of hierarchical Cs-pollucite nanocrystals.....	43
3.5	Characterizations techniques.....	44
3.5.1	X-ray powder diffraction (XRD) analysis	44
3.5.2	Fourier transform infrared (FTIR) spectroscopy	46
3.5.3	Solid-state magic-angle spinning nuclear magnetic resonance spectroscopy (MAS NMR)	48
3.5.4	Field emission scanning electron microscopy (FESEM)	49
3.5.5	Inductively coupled plasma optical emission spectroscopy (ICP-OES).....	51
3.5.6	Transmission electron microscopy (TEM).....	52
3.5.7	Nitrogen gas adsorption-desorption analysis.....	53

3.5.8	Thermogravimetry with derivative thermogravimetric (TGA/DTG) analysis.....	57
3.5.9	Temperature programmed desorption (TPD) analysis	58
3.5.10	Gas chromatography (GC) analysis	59
3.5.11	Gas chromatography-mass spectrometry (GC-MS) analysis.....	60
3.6	Catalytic Aldol condensation reactions study	60
CHAPTER 4 EFFECTS OF SYNTHESIS PARAMETERS ON THE FORMATION OF NANOCRYSTALLINE Cs-POLLUCITE.....		63
4.1	Introduction	63
4.2	Result and discussion	64
4.2.1	Effect of Cs ₂ O content.....	64
4.2.2	Effect of H ₂ O content	67
4.2.3	Effect of SiO ₂ content	70
4.2.4	Effect of type of mineralizer, MOH (M = Na, K, Cs)	73
4.2.5	Effect of Synthesis Temperature	75
4.3	Summary	78
CHAPTER 5 MICRO- AND MACROSCOPIC OBSERVATIONS OF THE NUCLEATION PROCESS AND CRYSTAL GROWTH OF NANOSIZED Cs-POLLUCITE IN ORGANOTEMPLATE-FREE HYDROSOL.....		79
5.1	Introduction	79
5.2	Results and discussion	80
5.2.1	Macroscopic study of the formation of nanosized Cs-pollucite.....	80
5.2.2	Microscopic study of the formation of nanosized Cs-pollucite.....	85
5.3	Nucleation process and crystal growth mechanism of nanosized Cs-pollucite.....	90
5.4	Summary	94

CHAPTER 6 CATALYTIC BEHAVIOUR OF Cs-POLLUCITE AS SOLID BASE CATALYST BY PERKIN CONDENSATION REACTION.....	95
6.1 Introduction.....	95
6.2 Results and discussion	95
6.2.1 Effect of reaction temperature and time	97
6.2.2 Effect of catalyst loading.....	98
6.2.3 Effect of benzaldehyde to acetic anhydride molar ratio	99
6.2.4 Effects of solvent.....	101
6.2.5 Catalyst comparative study.....	102
6.3 Effect of reaction heating modes.....	104
6.4 Catalyst reusability.....	104
6.5 Reaction mechanism	106
6.6 Summary	108
CHAPTER 7 HIERARCHICAL CS-POLLUCITE NANOZEOLITE MODIFIED WITH NOVEL ORGANOSILANE AS EXCELLENT SOLID BASE CATALYST FOR CLAISEN -SCHMIDT CONDENSATION OF BENZALDEHYDE AND ACETOPHENONE.....	109
7.1 Introduction.....	109
7.2 Results and discussion	110
7.2.1 Synthesis and characterization of hierarchical Cs-Pollucite nanozeolites.....	110
7.2.2 Catalytic reaction study	122
7.2.2(a) Effects of reaction temperature and time.....	122
7.2.2(b) Effect of catalyst loading.....	124
7.2.2(c) Effect of acetophenone to benzaldehyde molar ratio.....	125
7.2.2(d) Catalyst comparative study.....	126
7.3 Reaction mechanism	127
7.4 Summary	129

CHAPTER 8 CONCLUSIONS AND FUTURE WORKS	130
8.1 Conclusions	130
8.2 Recommendations of future works	132
REFERENCES	134
APPENDICES	
LIST OF PUBLICATIONS	

LIST OF TABLES

	Page
Table 2.1	Chemical sources and their respective functions in zeolite synthesis (van Bekkum <i>et al.</i> , 2001). 21
Table 2.2	Conversion of cinnamic acid in the presence of various catalysts under classic heat condition (Veverkova, Pacherova and Toma, 2010). 28
Table 2.3	Aldol condensation catalysed using of various solid acid and base catalysts under different conditions. 31
Table 3.1	The chemical compositions of hydrogels and the zeolite synthesis conditions. 42
Table 4.1	The crystals and particles size of samples. 78
Table 5.1	Si and Al elemental analysis of the solid products obtained after various heating times and synthesized using a hydrogel with a chemical compositions of 5.5 SiO ₂ :1Al ₂ O ₃ :6C ₂ S ₂ O:140H ₂ O 87
Table 6.1	Effect of solvent on Perkin condensation of benzaldehyde and acetic anhydride*. 101

LIST OF FIGURES

	Page
Figure 1.1	Representative structures of zeolites (Price, 2011). 2
Figure 2.1	The basic structure of zeolites, where the metal cation (M^+) neutralizes the negative charge of Al sites in the zeolite framework. 13
Figure 2.2	(a) The primary building unit (PBU) of zeolite structure in TO_4 (T = Al or Si) tetrahedral position, (b) some examples of the secondary building units of zeolites built by PBUs, and (c) the zeolites formed from the SBU units with their pore openings (Ghobarkar <i>et al.</i> , 1999; Weitkamp, 2000) 13
Figure 2.3	The properties of nanozeolites (Mintova, Grand & Valtchev, 2016). 19
Figure 2.4	Hydrothermal synthesis and purification processes of zeolite. 21
Figure 2.5	The synthesis of cinnamic acid by Perkin condensation of benzaldehyde and acetic anhydride. 27
Figure 2.6	The synthesis of chalcone by Claisen-Schmidt condensation of benzaldehyde and acetophenone. 30
Figure 2.7	Microwave dielectric heating via (a) migration of ionic atoms/molecules and (b) rotation of dipolar atoms/molecules (Kappe, 2004). 37
Figure 2.8	Non-microwave instant heating reactor (Obermayer <i>et al.</i> , 2016). 38
Figure 3.1	The appearance of precursor hydrogel for the synthesis of Cs-pollucite nanozeolite showing the white colloidal suspension 41
Figure 3.2	Synthesis scheme of hierarchical Cs-pollucite. 44
Figure 3.3	Types of adsorption isotherm curves (Sing <i>et al.</i> , 1985) 54
Figure 3.4	Types of hysteresis loops based on IUPAC classifications (Sing <i>et al.</i> , 1985). 55
Figure 4.1	XRD patterns of samples synthesized with the hydrogel molar composition of 5. $5SiO_2:1Al_2O_3: aCs_2O:140H_2O$ using different Cs_2O contents: (a) $a = 2.5$ (P1), (b) $a = 4$ (P2), (c) $a = 6$ (P3) and (d) $a = 8$ (P4) at 180 °C for 60 min. * indicates the presence of quartz crystalline phase. 65

Figure 4.2	FESEM images and particle size distributions of solids synthesized at 180 °C for 60 min using the hydrogel molar composition of 5. 5SiO ₂ :1Al ₂ O ₃ : aCs ₂ O:140H ₂ O with (a-e) a = 2.5 (P1), (b-f) a = 4 (P2), (c-g) a = 6 (P3) and (d-h) a = 8 (P4).....	66
Figure 4.3	XRD patterns of samples synthesized at 180 °C for 60 min using hydrogels with a chemical molar composition of 5. 5SiO ₂ :1Al ₂ O ₃ : 6Cs ₂ O:bH ₂ O where (a) b = 560 (P7) (b) b = 420 (P6) (c) b = 280 (P5), and (d) b = 140 (P3).	68
Figure 4.4	FESEM images of solids synthesized at 180 °C for 60 min using hydrogels with a chemical molar composition of 5. 5SiO ₂ :1Al ₂ O ₃ : 6Cs ₂ O:bH ₂ O where (a) b = 140 (P3), (b) b = 280 (P5), (c) b = 420 (P6) and (d) b = 560 (P7). The particle size distribution plots of P3 and P5 are shown in (e) and (f), respectively.	69
Figure 4.5	XRD patterns of powder samples obtained after 60 min at 180 °C using a hydrogel molar composition of dSiO ₂ :1Al ₂ O ₃ :6Cs ₂ O: 140H ₂ O where (a) c = 2.5 (P8), (b) c = 4 (P9), (c) c = 5.5 (P3) and (d) c = 7 (P10). * indicates the presence of quartz dense phase.	71
Figure 4.6	FESEM images and particle size distributions of samples obtained after 60 min at 180 °C using a hydrogel molar composition of dSiO ₂ :1Al ₂ O ₃ : 6Cs ₂ O:140H ₂ O where (a-e) d = 2.5 (P8), (b-f) d = 4 (P9), (c-g) d = 5.5 (P3) and (d-h) d =7 (P10).....	72
Figure 4.7	XRD patterns of samples synthesized with different metal hydroxides (MOH): (a) NaOH (P11), (b) KOH (P12) and (c) CsOH (P3) using a hydrogel molar composition of 5.5SiO ₂ :1Al ₂ O ₃ :6M ₂ O:140H ₂ O, 180 °C and 60 min of heating.	74
Figure 4.8	FESEM images of samples synthesized with different mineralizers: (a) NaOH, (b) KOH and (c) CsOH using a hydrogel molar composition of 5.5SiO ₂ :1Al ₂ O ₃ :6M ₂ O:140H ₂ O, 180 °C and 60 min of heating.	75
Figure 4.9	XRD patterns of pollucite samples synthesized with hydrogel of molar composition of 5.5SiO ₂ :1Al ₂ O ₃ : 6Cs ₂ O:140H ₂ O with different crystallization temperatures: (a) 160 °C (P13), (b) 170 °C (P14), (c) 180 °C (P3) and (d) 190 °C (P15) for 60 min.	76

Figure 4.10	FESEM images and particle size distribution histograms of pollucite samples synthesized with hydrogel of molar composition of $5.5\text{SiO}_2:1\text{Al}_2\text{O}_3:6\text{Cs}_2\text{O}:140\text{H}_2\text{O}$ heated at (a-e) 160 °C (P13), (b-f) 170 °C (P14), (c-g) 180 °C (P3) and (d-h) 190 °C (P15) for 60 min.	77
Figure 5.1	Solid yield after different heating times of hydrothermal treatment.....	81
Figure 5.2	XRD patterns of samples after (a) 15 min (P16), (b) 25 min (P17), (c) 30 min (P18), (d) 45 min (P19), (e) 60 min (P3) and (f) 120 min (P20).....	82
Figure 5.3	Crystallization rate of solid products after various heating times.	82
Figure 5.4	TEM images of samples after (a) 15 min (P16), (b) 25 min (P17), (c) 30 min (P18), (d, e) 60 min (P3) and (f, g, h) 120 min (P20). Inset of (d) is the theoretical shape of ANA crystalline solid while inset of (g) is the selected area electron diffraction (SAED) pattern of sample heated for 120 min.	84
Figure 5.5	IR spectra of solid products after hydrothermal synthesis for (a) 15 min (P16), (b) 25 min (P17), (c) 30 min (P18), (d) 60 min (P3) and (e) 120 min (P20).....	86
Figure 5.6	^{27}Al solid state MAS NMR spectra of samples heated after (a) 15 min (P16), (b) 25 min (P17), (c) 30 min (P18), (d) 60 min (P3) and (e) 120 min (P20).....	88
Figure 5.7	^{29}Si solid state MAS NMR spectra of samples heated after (a) 15 min (P16), (b) 25 min (P17), (c) 30 min (P18), (d) 60 min (P3) and (e) 120 min (P20).	90
Figure 5.8	Mechanism of the formation of nanosized Cs-pollucite zeolite. Inset: Framework structure of solid. Pink: Si or Al atom, and white: O atom. Cs atom is not shown.....	93
Figure 6.1	Perkin condensation of benzaldehyde with acetic anhydride catalysed by P2 (42.9 nm), P3 (29.9 nm), P4 (23.1 nm), P9 (69.4 nm) and P15 (33.7 nm) Cs-pollucite nanocrystals at 190 °C for 30 min (number of experiments, n = 2).	96
Figure 6.2	Perkin condensation of (1 mmol) benzaldehyde with (1.5 mmol) acetic anhydride without catalyst at (a) 170 °C, (b) 180 °C and (c) 190 °C, and with nanosized Cs-pollucite zeolite at (d) 170 °C, (e) 180 °C and (f) 190 °C (number of experiments, n = 2).....	97

Figure 6.3	Arrhenius plots of Perkin condensation of benzaldehyde performed (a) without and (b) with nanosized Cs-pollucite zeolite catalyst.....	98
Figure 6.4	Effect of catalyst amount on the benzaldehyde conversion in Perkin condensation where benzaldehyde: acetic anhydride molar ratio = 1:1.5, heating time = 30 min and reaction temperature = 190 °C were used (number of experiments, n = 2).....	99
Figure 6.5	Effect of benzaldehyde: acetic anhydride molar ratios on the benzaldehyde conversion in Perkin condensation where catalyst amount = 0.600 g, heating time = 30 min and reaction temperature = 190 °C were used (number of experiments, n = 2).....	100
Figure 6.6	Catalytic conversion to cinnamic acid catalysed with (a) sodium hydroxide, (b) potassium hydroxide and (c) nanosized Cs-pollucite zeolite. Benzaldehyde = 1 mmol, acetic anhydride = 1.5 mmol, catalyst amount = 0.600 g, reaction temperature = 190 °C, solvent-free (number of experiments, n = 2).....	103
Figure 6.7	Catalyst recycling test of nanosized Cs-pollucite zeolite in Perkin condensation reaction (number of experiments, n = 2).	105
Figure 6.8	XRD pattern of nanosized Cs-pollucite zeolite after 5 cycles of Perkin condensation reaction.	106
Figure 6.9	(a) FESEM and (b) TEM images of nanosized Cs-pollucite zeolite (P3) after 5 cycles of Perkin condensation reaction.	106
Figure 6.10	A proposed reaction mechanism of Perkin condensation between benzaldehyde and acetic anhydride catalyzed by Cs-pollucite solid base catalyst.	107
Figure 7.1	TG curves of as-synthesized (a) CP-0, (b) CP-0.3, (c) CP-1.0 and(d) CP-2.0.	111
Figure 7.2	²⁹ Si MAS + DEC NMR spectra of as-synthesized (a) CP-0 and (b) CP-2.0.	112
Figure 7.3	XRD patterns of calcined (a) CP-0, (b) CP-0.3, (c)CP-1.0 and (d) CP-2.0.	113
Figure 7.4	FESEM and particle size distributions of calcined (a-c) CP-0, (d-f) CP-0.3, (g-i) CP-1.0 and (j-l) CP-2.0.	114
Figure 7.5	IR spectra of calcined (a) CP-0, (b) CP-0.3, (c) CP-1.0 and (d) CP-2.0.....	115

Figure 7.6	Nitrogen gas adsorption (closed symbols) and desorption (open symbols) curves of (a) CP-0, (b) CP-0.3, (c) CP-1.0 and (d) CP-2.0. Inset: Pore size distribution derived from DFT method.	116
Figure 7.7	TPD-CO ₂ of (a) CP-0, (b) CP-0.3, (c) CP-1.0 and (d) CP-2.0.....	119
Figure 7.8	Correlation plots between the amount of TPOAC added with the specific surface area (S_{BET}) and basicity of Cs-pollucite samples.....	121
Figure 7.9	(A) Claisen-Schmidt condensation of benzaldehyde and acetophenone catalyzed with (a) CP-0, (b) CP-0.3, (c) CP-1.0 and (d) CP-2.0 nanocatalysts at 200 °C where the respective Arrhenius linear plots are also shown in (B) using the second-order rate constants determined at 180 °C, 190 °C and 200 °C (number of experiments, n = 2).....	123
Figure 7.10	Effect of catalyst loading on the conversion of Claisen-Schmidt condensation of benzaldehyde and acetophenone. Catalyst = CP-2.0, reaction temperature = 200 °C, reaction time = 100 min, benzaldehyde = 10 mmol, acetophenone = 5 mmol, solvent-free (number of experiments, n = 2).	124
Figure 7.11	Effect of acetophenone: benzaldehyde molar ratio on the conversion of Claisen-Schmidt condensation. Catalyst = CP-2.0, catalyst loading = 0.50 g, reaction temperature = 200 °C, reaction time = 100 min, solvent-free (number of experiments, n = 2).....	125
Figure 7.12	(A) Conversion of acetophenone in Claisen-Schmidt condensation reaction using different catalysts (reaction temperature = 200 °C, time = 100 min, benzaldehyde = 10 mmol, acetophenone = 5 mmol), and (B) catalyst reusability test of CP-2.0 in Claisen-Schmidt condensation of benzaldehyde and acetophenone (number of experiments, n = 2).....	127
Figure 7.13	A proposed reaction mechanism of aldol condensation between benzaldehyde and acetophenone over hierarchical Cs-pollucite solid base catalyst	128

LIST OF SYMBOLS AND NOMENCLATURES

ANA	Analcime topology
BET	Brunauer-Emmet-Teller
BJH	Barrett-Joyner-Halenda
ca.	Circa (approximately)
DTG	Derivative thermogravimetry
D8R	Double eight rings
D10R	Double ten rings
D12R	Double twelve rings
FESEM	Field emission scanning electron microscopy
FTIR	Fourier transform infrared spectroscopy
GC	Gas chromatography
HRTEM	High resolution transmission electron microscopy
IUPAC	International Union of Pure and Applied Chemistry
IZA-SC	International Zeolite Association Structure Commission
MAS NMR	Magic angle spinning nuclear magnetic resonance
MS	Mass spectrometry
M	Molarity
PBU	Primary building unit
E_T^N	Polarity scale
PP	Polypropylene
SBU	Secondary building unit
SAED	Selected area electron diffraction
SDAs	Structure-directing agents
TGA	Thermogravimetry analysis

TEM	Transmission electron microscopy
V_{total}	Total pore volume
XRD	X-ray diffraction
wt%	Weight percentage

SINTESIS NANOZEOLIT Cs-POLLUSIT DAN KAJIAN PEMANGKINAN DALAM TINDAK BALAS KONDENSASI DIMANGKINKAN BES

ABSTRAK

Projek ini bertujuan untuk mensintesis pemangkin pepejal Cs-pollusit (topologi ANA) tanpa agen pengarah struktur organik untuk tindak balas kondensasi benzaldehid. Bahagian pertama memberi tumpuan kepada kesan parameter sintesis (misalnya suhu pemanasan, masa dan komposisi kimia hidrogel) terhadap proses penghabluran zeolit Cs-pollusit nanohablur. Beberapa sifat seperti ketulenan produk pepejal, taburan saiz hablur dan morfologi didapati dipengaruhi oleh perubahan dalam parameter sintesis. Selain itu, kajian induksi, penghabluran dan pertumbuhan hablur zeolitCs-pollusit nanohablur daripada prekursor tanpa acuan organik $5.5\text{SiO}_2: 1\text{Al}_2\text{O}_3: 6\text{Cs}_2\text{O}: 140\text{H}_2\text{O}$ juga dilaporkan dan pelbagai teknik spektroskopi, mikroskopi dan analisis digunakan untuk mengikuti keseluruhan proses penghabluran. Pepejal sampel pada mulanya mengalami pengorganisasian semula fasa amorfus sebelum nukleasi (25 min), penghabluran (60 min) dan pertumbuhan hablur (120 min) berlaku. Nanohablur Cs-pollusit yang dihasilkan (purata saiz 55 nm) memaparkan morfologi trapezohedron dan hablur tersebut boleh distabilkan secara koloid dalam air. Bahagian ketiga projek ini ditujukan kepada penggunaan organosilana baharu, iaitu dimetiloktadesil [3-(trimetoksisilil)propil] ammonium klorida (TPOAC), sebagai agen pembesaran liang yang berkesan dalam pembentukan struktur hierarki dalam nanosaiz Cs-pollusit. Untuk mendedahkan peranan TPOAC dalam proses penghabluran Cs-pollusit, empat kandungan TPOAC yang berbeza telah ditambah semasa sintesis hierarki Cs-pollusit (CP- x , $x = 0, 0.3, 1.0$ atau 2.0 dengan x adalah nisbah molar TPOAC). TPOAC telah menunjukkan perubahan sifat fiziko-kimia dan morfologi nanosaiz Cs-pollusit, seperti

mengurangkan kehabluran, saiz hablur yang lebih kecil, taburan saiz liang yang lebih besar, luas permukaan dan isipadu liang yang lebih tinggi dengan kebesaran permukaan yang meningkat (bilangan tapak dan kekuatan). Akhir sekali, penyelidikan ini juga mengkaji prestasi pemangkinan Cs-pollusit nanopepejal dalam tindak balas bermangkinkan bes. Bagi nanosaiz Cs-pollusit, kondensasi Perkin benzaldehid dan asetik anhidrida di bawah keadaan pemanasan segera bukan gelombang mikro digunakan untuk menilai kelakuan pemangkinnya dan beberapa parameter tindak balas pemangkinan telah diubah dan dikaji. Kajian menunjukkan bahawa nanosaiz Cs-pollusit mencapai penukaran tindak balas tertinggi (82.9%) dengan 100% keterpilihan terhadap sinamik asid di bawah keadaan yang optimum (190 °C, 30 min, nisbah tindak balas 1:1.5, muatan mangkin 0.6 g) dan prestasi pemangkinnya adalah lebih baik daripada pemangkin KOH dan NaOH. Bagi nanomangkin hierarki zeolit Cs-pollusit, kondensasi Claisen-Schmidt benzaldehid dan asetofenon di bawah keadaan pemanasan segera bukan gelombang mikro digunakan sebagai tindak balas model untuk menguji prestasi pemangkinan pepejal tersebut. Hasil kajian menunjukkan bahawa hierarki Cs-pollusit (CP-2.0) menunjukkan penukaran tindak balas yang lebih baik (82.2%) kepada chalkon (kepilihan 100%) berbanding nanosaiz Cs-pollusit biasa (CP-0) (100% kepilihan terhadap chalkon). Nanomangkin hierarki CP-2.0 juga menunjukkan prestasi pemangkinan yang lebih baik daripada mangkin homogen dan heterogen yang lain, seperti NaOH, Na₂CO₃, KOH, CsOH, dan NaX, dan mangkin tersebut mempunyai kebolehgunaan semula yang tinggi tanpa kemerosotan yang ketara dalam prestasi pemangkinan walaupun selepas lima kitaran tindak balas yang berturutan.

**SYNTHESIS OF Cs-POLLUCITE NANOZEOLITE
AND CATALYTIC STUDY IN BASE-CATALYZED BENZALDEHYDE
CONDENSATION REACTIONS**

ABSTRACT

This project aims to synthesize nanosized Cs-pollucite (ANA topology) solid catalyst without organic structure-directing agent for condensation reactions of benzaldehydes. The first part focuses on the effect of the synthesis parameters (e.g. heating temperature, and hydrogel chemical composition) on the crystallization process of nanosized Cs-pollucite zeolites. Several properties such as the purity of the solid products, crystal size distribution and morphology are affected upon changing the synthesis parameters. Besides, time-dependent study of induction, nucleation and crystal growth of nanoscaled Cs-pollucite zeolite from an organotemplate-free precursor suspension of $5.5\text{SiO}_2:1\text{Al}_2\text{O}_3:6\text{Cs}_2\text{O}:140\text{H}_2\text{O}$ is also reported where various spectroscopy, microscopy and analytical techniques are used to follow the entire crystallization process. The solid initially experienced amorphous phase re-organization before nucleation (25 min), crystallization (60 min) and crystal growth (120 min) took place. The resulting Cs-pollucite nanocrystals (average size 55 nm) displayed trapezohedron morphology and they can be colloidally stabilized in water. The third part of this project is dedicated to the use of new organosilane, *viz.* dimethyloctadecyl[3-(trimethoxysilyl)propyl] ammonium chloride (TPOAC), as a promising pore expanding agent to develop the hierarchical structure in nanosized Cs-pollucite. In order to reveal the roles of TPOAC in the crystallization process of Cs-pollucite, four different amounts of TPOAC were added during the synthesis of hierarchical Cs-pollucite (CP- x , $x = 0, 0.3, 1.0$ or 2.0 where x is the molar ratio of

TPOAC). TPOAC has shown to alter the physico-chemical and morphological properties of nanosized Cs-pollucite, such as reduced crystallinity, smaller crystallite size, larger pores size distribution, higher surface areas and pore volumes with improved surface basicity (amount and strength). Finally, this work also studies the catalytic performance of Cs-pollucite nanosolids in base-catalyzed reactions. For nanosized Cs-pollucite, Perkin condensation of benzaldehyde and acetic anhydride under non-microwave instant heating conditions was used to evaluate its catalytic behavior where several catalytic reaction parameters were adjusted. The study shows that nanosized Cs-pollucite achieved the highest reaction conversion (82.9%) with 100% selective to cinnamic acid under optimized conditions (190 °C, 30 min, reaction ratio 1:1.5, catalyst loading (0.6 g) and its catalytic performance is better than KOH and NaOH catalysts. For hierarchical Cs-pollucite zeolite nanocatalyst, Claisen-Schmidt condensation of benzaldehyde and acetophenone under non-microwave instant heating condition was used as a model reaction to test the catalytic performance of the catalyst. The results reveal that hierarchical nanosized Cs-pollucite (CP-2.0) showed the improved reaction conversion (82.2%) to chalcone (100% selectivity) as compared to common nanosized Cs-pollucite (CP-0) which only achieves 68.5% conversion (100% selective to chalcone). The hierarchical CP-2.0 nanocatalyst also shows better catalytic performance than other homogenous and heterogeneous catalysts, such as NaOH, Na₂CO₃, KOH, CsOH, and, NaX, and it has high catalyst reusability with no significant deterioration in catalytic performance even after five consecutive reaction runs.

CHAPTER 1

INTRODUCTION

1.1 General introduction

Nanoporous solids are very interesting materials. Because of their specific characteristics such as high accessible porosity, large surface area, adjustable structures, they have been used as catalysts, adsorbents, molecular sieves and ion exchangers in fine chemical industries. The pore size of nanoporous materials can be classified into three different classes based on their pore diameter (\emptyset) as adopted by the International Union of Pure and Applied Chemistry (IUPAC) (Sing *et al.*, 1985): micropores where $\emptyset < 2.0$ nm, mesopores where $2.0 < \emptyset < 50$ nm, and macropores where $\emptyset > 50$ nm.

Zeolites are crystalline microporous materials which are widely used as catalysts, particularly in the petrochemical industry. They have three dimensional and well-defined structures composed of aluminium, silicon and oxygen elements. In the zeolite frameworks, the basic building units of zeolites are TO_4 tetrahedra (T = Si or Al). Pure siliceous zeolite has neutral charge surface. However, the framework will bear a negative charge when the T atom is replaced with an Al atom (Motsi *et al.*, 2009), and this negative charge is counter-balanced by the non-framework cations (Na^+ , K^+ , Cs^+ or H^+) in order to maintain the electrical neutrality of the framework (Price, 2011).

The zeolite structures have channels and/or cages of approximate size of 0.3 to 1.5 nm. Usually, zeolites can be divided into three classes (Figure 1.1), namely small pore zeolites with eight membered-ring pore apertures having pore opening of 3.0 to 4.5 Å (e.g. zeolite A), medium pore zeolites with ten membered-ring apertures of pore

opening of 4.5 to 6.0 Å (e.g. zeolite ZSM-5), and large pore zeolites with twelve membered-ring apertures having a pore diameter of 6.0 to 8.0 Å (e.g. zeolite Beta and zeolite Y). Since the first zeolite found in 1756, there are about 250 types of zeolite frameworks that have been recognized by the International Zeolite Association (IZA) up to now (Baerlocher and McCusker, 2019) where 40 types of structures can be found in nature (Hovhannisyan *et al.*, 2018).

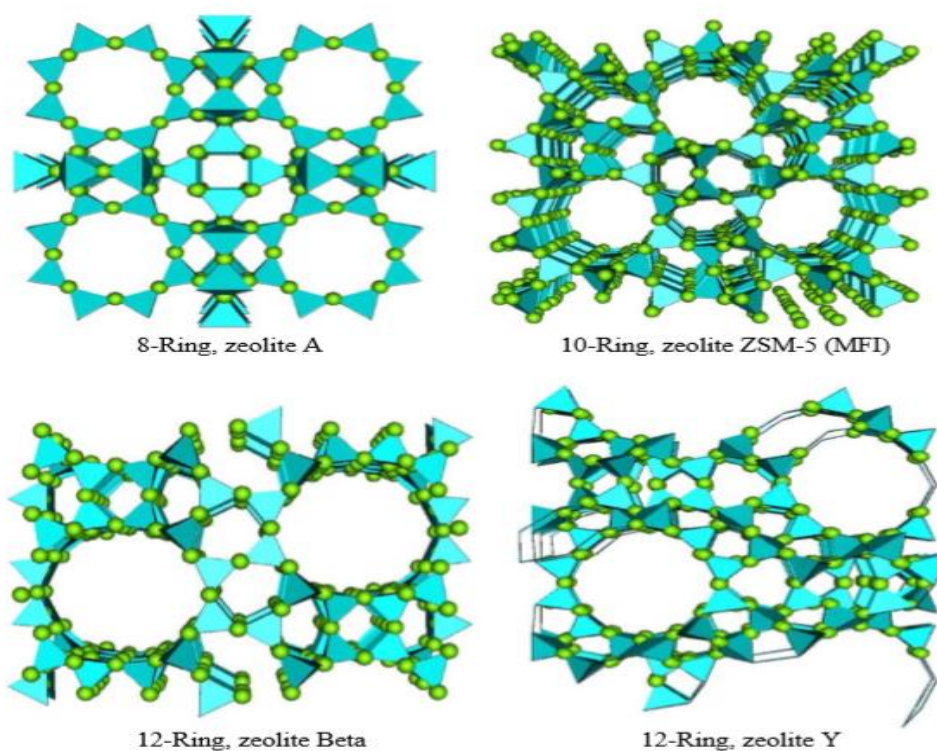


Figure 1.1. Representative structures of zeolites (Price, 2011).

Generally, natural zeolites can also be prepared industrially in large scale. Some of the common zeolite minerals are analcime, heulandite, stilbite, chabazite, natrolite, phillipsite and clinoptilolite. Naturally occurring zeolites are usually not pure due to the presence of other contaminants such as other minerals, rocks and metals. As a result, naturally occurring zeolites are seldom used in many important commercial

applications, and hence, many important synthetic zeolites are produced for meeting the needs of industries (Chipera and Apps, 2001).

The synthetic zeolites do not alter their characteristics under elevated temperatures and pressure. Moreover, synthetic zeolites show very small toxicity effect to the living organisms (Kasperkowiak *et al.*, 2016). Such properties allow zeolites to be more preferable than other porous materials used in industries as catalysts (Amodul *et al.*, 2015), biomedical agents (Anderson *et al.*, 2017), environmental adsorbents to remove heavy metals from sewage (Bashir *et al.*, 2018) and agricultural fertilizer. The appropriate applications of zeolites mainly depend on the pore size, pore dimension, crystal shape and crystal size of the zeolites (Moliner *et al.*, 2015). However, the great barriers of zeolites in catalytic application is the diffusion of bulky reactant molecules in their micropores which might lead to pore blockage and catalyst deactivation. In order to solve this problem, several strategies are adopted to fix this issue (Mintova *et al.*, 2016).

In recent years, mesoporous molecular sieves with well-defined and larger pore sizes of 2 to 50 nm have received much attention (Zhu *et al.*, 2011). The larger pores of mesoporous materials can be an alternative in solving the catalytic reaction problem faced by zeolites. However, mesoporous materials usually have lower acidity or basicity due to their amorphous pore walls. In addition, they have low hydrothermal and chemical stabilities than traditional zeolites. Therefore, any effort to improve the properties of mesoporous materials (improved diffusion rate, high acidity or basicity, and high hydrothermal stability and resistance to harsh chemical environment) are urgently needed.

The synthesis, characterization and applications of nanosized zeolites (<100 nm) gain great attention recently due to their unusual properties such as reducing diffusion path length, high colloidal stability, large external surface and low toxicity (Wong *et al.*, 2017; Huang *et al.*, 2017). As a result, the nanozeolites have expanded the field of zeolite applications towards medicine (Laurent *et al.*, 2013), electronics (Mercedes *et al.*, 2005), energy storage (Gopal *et al.*, 1982), drug delivery (Shan *et al.*, 2006), paints (Tong *et al.*, 2015) optical layers materials (Tosheva *et al.*, 2008) lubricants (Maiano *et al.*, 2011). Unlike mesoporous materials, nanosized zeolites are more hydrothermally and chemically stable due to their crystalline pore walls similar to their micron-sized counterparts.

Zeolite nanocrystals are usually synthesized from clear solution of aluminosilicates in the presence of organic templates (amine, imidazolium or quaternary ammonium salts) (Ng *et al.*, 2014; Song *et al.*, 2005). The addition of organic templates in the precursor synthesis gel is important to control the size of crystals besides these additives help in forming the specific crystalline framework (Mintova *et al.*, 1995). However, the use of organic templates in the synthesis of nanozeolites gives many disadvantages. First, the nanozeolites may face irreversible aggregation after the removal of organic templates by calcination at elevated temperatures. Second, the application of organic templates in the synthesis of nanozeolite causes a variation in the Si and Al framework composition. For instance, nanozeolite A with a Si/Al ratio above 1 is obtained when organic template is used, whereas nanozeolite A with a Si/Al ratio of 1 is produced when no organic template is added. Third, the organic template is expensive and environmentally unfriendly (Duan *et al.*, 2018; Cui *et al.*, 2017). During the removal of organic templates *via* high-temperature calcination, toxic gases such as volatile amines are also released which

will also harm the human health. Hence, zeolite nanocrystals with eco-friendly and cheaper preparation protocols are needed. So far, ionothermal technique (Parnham *et al.*, 2007) organo-template-free approach (Wong *et al.*, 2017) space confinement synthesis (Madsen and Jacobsen, 1999) and seeding method (Kamimura *et al.*, 2010) have been used to replace the traditional organo-templating approach for synthesizing nanosized zeolites.

In general, microporous and mesoporous materials are synthesized in the form of Na⁺ and/or K⁺. For instant, FAU- and SOD-typed zeolites are crystallized in sodium-rich precursors (Oleksiak, M. D. & Rimer, 2014 and Ogura *et al.*, 2003) while zeolites of LTL and LTJ structures are formed in potassium-rich aluminosilicate hydrogels (Ahmad *et al.*, 2020 and Thomas *et al.* 2017). However, the synthesis of Cs-based zeolites is very rarely reported due to their extreme synthesis conditions that require very high crystallization temperature (200-300 °C) and pressure (300-850 bar) (Chen *et al.*, 2018; Yokomori, 2014). As a result, the formation mechanism of Cs-based zeolites is not clear up to now and it is still a great challenge for zeolite researchers to understand the behaviour of the zeolites. In addition, the preparation of zeolite nanocrystals based on cesium using this method has never been documented so far. It is because the synthesis of zeolite nanocrystals is a complicated process as it is influenced by many variables including synthesis temperature, crystallization time, type of mineralizer and its concentration, water content, aging treatment and heating mode. Therefore, it is worth to further do a comprehensive study on the synthesis of cesium-based nanozeolites and investigation of nucleation and crystallization stages. So far, only two types of Cs-based zeolites are discovered, namely pollucite and ABW. Among these two Cs-zeolites, only pollucite can be found in nature and the crystals are usually very huge (>5 µm). Compared to ABW-type zeolite, pollucite is more

interesting because it has three-dimensional more open channel with 8-membered ring pore size (pore opening 2.43 Å) forming ANA framework structure (Mintova *et al.*, 2016). Unlike Na and K-zeolites, zeolite containing Cs⁺ cation is more interesting due to its highly basic property that is appreciated in base-catalyzed reactions (heterogeneous catalysis). In addition, it can be reused without loss of reactivity even after several consecutive runs (Ng *et al.*, 2019). However, no research work has been reported so far on the use of Cs-pollucite in this catalytic application. This might be due to the fact that the micropores of Cs-pollucite is too small for enabling bulky molecular reactants to diffuse and react in its micropore channels where most of the active sites are located in the micropores of the zeolite.

In this study, the synthesis of Cs-pollucite in mild and safer condition (particularly for nanometer-sized crystals) with lower crystallization temperature and pressure with ANA topology in cesium-rich and organotemplate-free medium is reported. The mechanism of the induction, nucleation and crystal growth of Cs-pollucite zeolite nanocrystals and investigate the effects of zeolite synthesis parameters including initial molar composition synthesized in template free of Al₂O₃-SiO₂-Cs₂O-H₂O precursor system. In addition, modified the pore by synthesis hierarchical Cs-pollucite (micro/macropores) in order to overcome the diffusion of limitation of bulky molecules in Cs-pollucite by using surfactant (TPOAC) templating techniques. Lastly, the catalytic behavior of Cs-pollucite nanozeolite and hierarchical Cs-pollucite in base-catalyzed reactions such as Perkin condensation and Claisen-Schmidt condensation under non-microwave instant heating condition are tested.

1.2 Research objectives

There are four main objectives in this project which are shown as follows:

- a) To determine the effects of synthesis parameters (i.e. reaction time, reaction temperature, concentrations of CsOH, H₂O and SiO₂) on the crystallization of Cs-pollucite zeolite.
- b) To evaluate the nucleation and crystal growth of Cs-pollucite zeolite nanocrystals free of organic template under hydrothermal condition using microscopy and spectroscopy techniques.
- c) To examine the effects of organosilane on the generation of micro/macropores in Cs-pollucite zeolite.
- d) To study the catalytic properties of synthesized Cs-pollucite zeolite solids in base-catalysed reactions such as Perkin condensation of acetic anhydride and benzaldehyde, and aldol condensation (Claisen-Schmidt condensation) of acetophenone and benzaldehyde under non-microwave instant heating condition.

1.3 Overview of the thesis

This thesis consists of eight chapters, which generally covers a brief explanation of the project background, literature study on this research, experimental procedures and research finding of the project. Chapter 1 describes the introduction clarifying the definition and properties of zeolite materials. In this chapter, the problems statement and the intentions of this project are also discussed. Chapter 2 is a comprehensive literature review of the general aspects related to the field of project study covering the description of the history of zeolite, zeolite framework structures

and their properties, the fundamental synthesis concept of microporous and mesoporous materials, the fundamentals of characterization techniques and the applications of zeolite materials particularly in heterogeneous catalysis.

Chapter 3 presents the experimental methodology used in this entire project, which covers the study of the effects of synthesis parameters on the formation of Cs-pollucite, the nucleation and crystallization of nanosized Cs-pollucite. In addition, the experimental protocol for two base-catalytic reactions, namely Perkin condensation of benzaldehyde and acetic anhydride and aldol condensation (Claisen-Schmidt condensation) of benzaldehyde and acetophenone, and the measurement details of various characterization techniques are also reported in this chapter.

Chapter 4 reports the results of the effects of synthesis parameters on the formation of Cs-pollucite nanocrystals (ANA topology) in organotemplate-free system. Five synthesis parameters such as heating temperature, concentration of CsOH, water and SiO₂ content are adjusted in order to observe each parameter on the crystallization kinetics, degree of crystallinity, morphology, crystal size and purity of Cs-pollucite zeolite.

Chapter 5 presents the results of nucleation and crystallization of nanosized Cs-pollucite which are performed in organotemplate-free hydrogel system. The zeolite synthesis is conducted under hydrothermal treatment at various times where induction, nucleation and crystal growth are observed. Besides, the crystal growth mechanism of Cs-pollucite zeolite nanocrystals is also proposed in this chapter mainly based on the microscopic and spectroscopic observations.

Chapter 6 reports the findings of the catalytic performance of Cs-pollucite nanozeolite in base-catalysed Perkin condensation reaction of benzaldehyde and acetic

anhydride. In this reaction, novel non-microwave instant heating is used instead of conventional reflux method. The effects of catalytic reaction parameters such as heating time, heating temperature, reactant ratio, catalyst loading, solvent effect and mode of heating are also discussed.

Chapter 7 is dedicated to the modification of Cs-pollucite zeolite by creating micro/macroporous structure in it through using different contents of organosilane meso-templating agent, namely [3-(trimethoxysilyl)propyl] octadecyldimethylammonium chloride (TPOAC). The resulting solids are then systematically characterized with various instruments to reveal the surfactant roles in the synthesis. Then, the Cs-pollucite zeolite with hierarchical porosity is tested in the aldol condensation (Claisen-Schmidt condensation) of acetophenone and benzaldehyde reaction under non-microwave instant heating condition where the influences of each catalytic reaction parameter is also investigated.

Lastly, Chapter 8 presents the summary of the research findings and conclusion of this project. Moreover, some recommendations for the future works of this research are also proposed.

CHAPTER 2

LITERATURE REVIEW

2.1 Introduction

Zeolites or so-called molecular sieves are a class of porous materials with unique and selective adsorption and catalytic characteristics that strongly depends on their porous properties (e.g. pore size, shape, etc.). As a result, they can be used in many applications such as separation and catalysis. Zeolites are a common microporous crystalline material which have pore sizes less than 2 nm where zeolites, aluminophosphate zeotypes and metal organic frameworks (MOF) are described under the class of microporous molecular sieves.

2.2. Discovery and history of zeolites

Zeolite history began in 1756 when a Swedish mineralogist, Alex Fredrick Crönstedt, found the first known mineral, called stilbite (Serrano and Grieken, 2001). He found that when the mineral stilbite was quickly heated in a pipe flame, huge quantity of occluded water which was adsorbed by the mineral was released (Ramesh and Reddy, 2011). Therefore, this new mineral had been coined as "zeolite" which was derived from two classic Greek names, *zeo* and *lithos*, which means rock and boiling, respectively, because the mineral stone looked boiling when it was heated at approximately 200°C (Ramesh and Reddy, 2011). He then classified zeolites as a new group of minerals consisting of alkaline earth and alkaline aluminosilicates.

In 1857, Damour showed the hydration-dehydration properties of zeolites (van Bekkum, Flanigen, Jacobs and Jansen, 2001). In 1925, Weigel and Steinhof managed

to separate the gas molecules by their volume by separating the water molecules from the inner zeolite structure. In 1927, Leonard first identified the zeolite mineral with X-ray diffraction (Leonard, 1927). In 1930, Taylor and Pauling identified the first single crystal structure of zeolite minerals (Taylor, 1930; Pauling, 1930). In 1938, Barrer successfully synthesized chabazite and mordenite which were good materials for industrial air purification and separation. In the 1950s, Milton and his friend, Donald W. Breck, discovered more commercially valuable zeolites, namely zeolites A, X, and Y. The zeolites were then used in industrial purification and separation in 1954 as selective adsorbents and catalysts. Zeolites were found to have various unique characteristics, including strong catalytic, cation exchangeable and adsorption properties, as well as high hydration property (van Bekkum *et al.*, 2001; Szostak, 1992).

Zeolites are now known for their industrial applications. Naturally, zeolites are formed when volcanic rocks and ash layers react with alkaline soil waters. When the resulting aluminosilicate minerals are deposited for thousands to millions of years in shallow marine environments, zeolites are crystallized and formed. So far, there are about 40 natural zeolites have been discovered (Othmer, 1984). Some examples of natural zeolites are chabazite, analcime, erionite, mordenite, clinoptilolite, etc. Natural zeolites are usually cheap but are seldom in pure condition due to the contamination of other metals, minerals, etc. As a result, natural zeolites become less desirable in many important commercial applications, where purity is mattered.

Until today, about 250 types of zeolites have been successfully identified by the Structure Commission of the International Zeolite Association (IZA) where three-letter code, for example, FAU, EMT, MFI, LTJ, CHA, etc., are assigned to each system structure. In comparison to the natural zeolites, synthetic zeolites, which are

synthesized in the laboratory, have many advantages, such as high purity, uniform pore distribution and better ion exchange property (Szostak, 1992). Particularly, the synthesized zeolites—X, Y, A and ZSM-5—are widely used in many potential industrial applications due to their distinct ion exchange, adsorption and catalytic properties.

2.3 Structure of zeolites

Zeolites are hydrated and porous crystalline materials. These aluminosilicates have unique framework structures built up of silica (SiO_2) and alumina (AlO_2)⁻ tetrahedral units where the O atoms connect the inorganic tetrahedral units (Ghobarkar *et al.*, 1999; Weitkamp, 2000). When the framework is only constructed by tetrahedral SiO_2 , the overall framework charge is zero (neutral). However, when Al^{3+} is incorporated in the zeolite silicate framework in $[\text{AlO}_2]^-$ tetrahedral form, the surface charge now changes to negative (-1) where extra-framework cations (organic or metal cation) are needed to counter-balance and maintain the general framework neutrality (Figure 2.1). As a result, it creates a strong electrostatic field on the surface of zeolites (Payra and Dutta, 2003; Flanigen, 2001).

The zeolite structure consists of cages and interconnected voids of distinct sizes which are often filled with water molecules and charge balancing extra-framework cations (Doula and Dimirkou, 2006). These cations are mobile and exchangeable. The adsorbed water molecules can be removed reversibly using heat (Jacobs *et al.*, 2001). Equation 2.1 describes the empirical formula of zeolites (Petrov and Michalev, 2012):



where M is the exchangeable metal cation of valence n (from Group 1 or 2), while a , b and c are the numbers of mol.

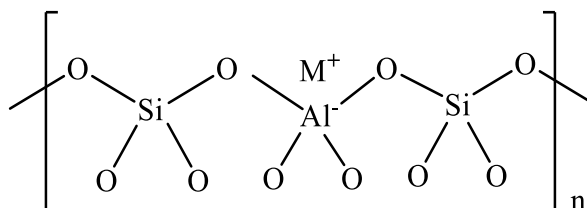


Figure 2.1. The basic structure of zeolites, where the metal cation (M^+) neutralizes the negative charge of Al sites in the zeolite framework.

In general, zeolite structures are built by primary and secondary building units. The primary building units (PBU) are the simplest building blocks which form the secondary building units (SBU) (Figure 2.2).

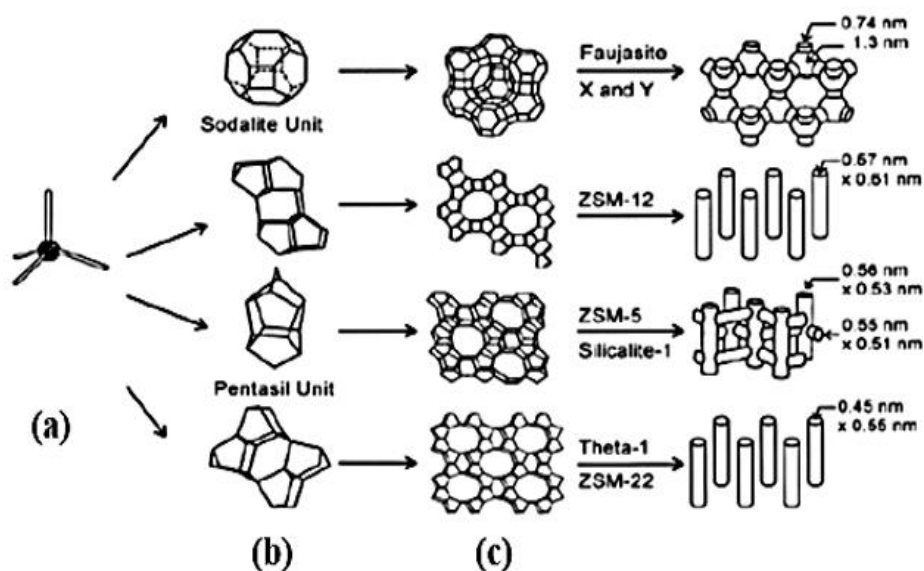


Figure 2.2. (a) The primary building unit (PBU) of zeolite structure in TO_4 ($T = Al$ or Si) tetrahedral position, (b) some examples of the secondary building units of zeolites built by PBUs, and (c) the zeolites formed from the SBU units with their pore openings (Ghobarkar *et al.*, 1999; Weitkamp, 2000).

Usually, zeolites are prepared in aluminosilicate form. Nevertheless, other tetrahedral elements such as tin (Vaughan and Rice, 1990), boron (Coudurier *et al.*, 1987), gallium (Fricke *et al.*, 2000) and germanium (Hu *et al.*, 2014) can also be incorporated into the zeolite framework, forming titanosilicate, borosilicate, gallosilicate, and germanosilicate zeotype materials.

2.4 Effect of synthesis parameters on the formation of zeolites

There are several factors affecting the zeolite formation during the synthesis process including time and temperature of crystallization, mineralizing agents, water, Si/Al ratio and alkalinity. They play a role in defining the type, morphology and topology, and impact on properties of zeolite as well. To synthesize and evaluate zeolite behavior, the most essential to control those factors.

2.4.1 Alkalinity

Zeolites are usually synthesized under basic requirements, where the degree of basicity depends on the OH⁻/Si and H₂O / Na₂O molar ratios. An important parameter is the alkalinity because it controls the solubilization of Si and Al sources. A rise in alkalinity results in a rise in the solubility of Si and Al sources and accelerates the polymerization of Si and Al sources. Furthermore, the high alkalinity of the precursor hydrogels often speeds induction and nucleation rates, and then accelerates zeolite crystallization (Xu *et al.*, 2007). As a consequence, zeolite crystals with smaller crystallite size and large particle size distribution are formed (Johnson and Arshad, 2014). In addition, for the crystallization of Al-rich zeolites (Si /Al ratio < 2) such as FAU, ABW, SOD and GIS typed zeolites, precursor solutions with strong alkalinity

are necessary. On the other hand, zeolites are very rarely crystallized under acidic conditions, as high pH is needed to dissolve sources of Al and Si (Dou *et al.*, 2010).

2.4.2 Effect of temperature

The synthesis temperature affects not only the crystals growth rate but also the solid yield and the morphological properties of zeolites (Auerbach *et al.*, 2003). The temperature variation effect is important as it affects the polymerization reaction between aluminate and polysilicate species. By increasing the synthesis temperature, the polymerization rate between the two inorganic species is increased (Xu *et al.*, 2007). Additionally, an increase in temperature also shortens the nucleation and induction time (Khajavi *et al.*, 2010). As a consequence, zeolites can be collected at a shorter time when the zeolite is crystallized at higher temperature. However, the size of the crystals often increases as the synthesis temperature rises.

2.4.3 Effect of time

The crystallization time influences greatly on the purity and quality of zeolites produced. There is also a clear relationship between the temperature of synthesis and the heating time. For instance, low-temperature zeolite synthesis requires longer time to form zeolite crystals, and vice versa (Johnson and Arshad, 2014). Ogura *et al.* prepared zeolite-type FAU for 24 h at 90 °C (Ogura *et al.*, 2003). Other phases of zeolite, such as chabazite (CHA), sodalite (SOD), and analcime (ANA), were also observed when the synthesis time was extended to 48 h further. Similarly, Ng *et al.* prepared the EMT-type zeolite for 36 h at very low temperature (30 °C) and, with extended synthesis time, led to the formation of zeolite type SOD (Ng *et al.*, 2012).

Hence, efficient control of crystallization time has to be taken into consideration when the synthesis of zeolite is carried out.

2.4.4 Effect of mineralizing agents (OH⁻)

Hydroxide concentration (OH⁻) plays an important role in the entire zeolite crystallization process. It affects not only on the rate of crystallization but also the crystal size and the zeolite type produced. Increasing the concentration of OH⁻ is expected to result in an increase in the solubility of silica and aluminum where high solubility of inorganic sources increases the supersaturation level of the solution which further increases the nucleation and crystal growth levels within a short time (Feng *et al.* 2016). Some additional phases of zeolite can co-crystallize together with the desired zeolite phase when the concentration of OH⁻ is not optimized. Therefore, determining the optimum quantity of OH⁻ is necessary where the quantity of OH⁻ is contributed by several sources such as silica, alumina, organic template and any additional alkali or alkali earth metal hydroxides (Cejka *et al.* 2017).

2.4.5 Effect of the Si/Al ratio

The Si/Al or SiO₂/Al₂O₃ ratio values in precursor hydrogels can be adjusted from 1 to certain (pure siliceous) values. It has very important influences on the zeolite structures, characteristics and sizes (Shalygin *et al.*, 2017). For example, the Si/Al ratio governs a zeolite's thermal stability, where its thermal stability is improved by increasing the ratio to ∞. However, the low silica zeolites (with a high Al content) are energetically unstable due to their high surface negative charge originated from the framework [AlO₄]⁻ species. As a result, high electrostatic repulsion forces in

framework structure is generated. In addition, the Si/Al ratio also affects the synthesis condition of zeolites. Aluminum-rich zeolites are typically prepared in precursor hydrogels with a low Si/Al ratio under a strong alkaline condition, whereas the silica-rich zeolites are prepared in a weak alkaline solution (Johnson and Arshad, 2014).

2.4.6 Effects of water content

In the hydrothermal synthesis of zeolites, water is essentially used as a solvent (Li & Liu, 2010). The amount of water influences the reactant concentration in the hydrogel solution, which thus impacting the size of the crystal and the yield of solid product. At low water content, it increases the mother liquor's supersaturation condition which affects the nucleation phase, and hence producing small-sized crystal particles. For example, in the synthesis of ZSM-5 zeolite, Sashkina *et al.* studied the effect of the H₂O/SiO₂ ratio (Sashkina *et al.*, 2017). The crystal size was significantly decreased from 1250 to 180 nm with reduced H₂O content in the hydrogel solution (reduced from 10 to 300 in the H₂O / SiO₂ ratio). Hence, the water content has to be controlled as low as possible when synthesizing nanosized zeolites.

2.5 Nanosized zeolites

Nanosized zeolites are zeolites which have crystallite size smaller than 100 nm (Knyazeva and Ivanova, 2019; Mintova, Gilson, and Valtchev, 2013). The decrease in crystal size is beneficial in most situations and it enhances the use of zeolites in various industrial applications. Figure 2.3 summarizes the beneficial effects of nanosized zeolites. The significant decrease in zeolite crystal sizes, however, could also have some negative effects. For example, under very mild conditions of synthesis, the

synthesized nanozeolite materials often exhibit a large number of defects in the framework structure. However, they display much larger external surface area than micron-sized zeolites. Large external surface areas are beneficial when it involves the diffusion and adsorption of bulky molecules that are difficult to pass through the zeolite pore window. Also, the short diffusion path over nanosized zeolites improves the reaction kinetics and limits the formation of coke, but zeolite selectivity on the other hand might be affected (Mintova, Grand & Valtchev, 2016)

In post-synthesis treatment, the technique used to purify nanosized zeolites is different from that of micron-sized crystals so that aggregation between the particles can be avoided. Normally, high-speed centrifugation and redispersion of zeolite nanoparticles in distilled water steps are used during purification of nanosized zeolites where the unreacted reactants are usually removed during washing and re-dispersion. The repetition of the both processes then change the pH of the resulting suspension to 7 or 8. At the end of the purification, the nanocrystals are in water suspension form with sufficiently high colloidal stability where the repulsive forces of negatively surface-charged nanocrystals protect the nanocrystals against aggregation for very long time (months to years) (Mintova, Grand & Valtchev, 2016).

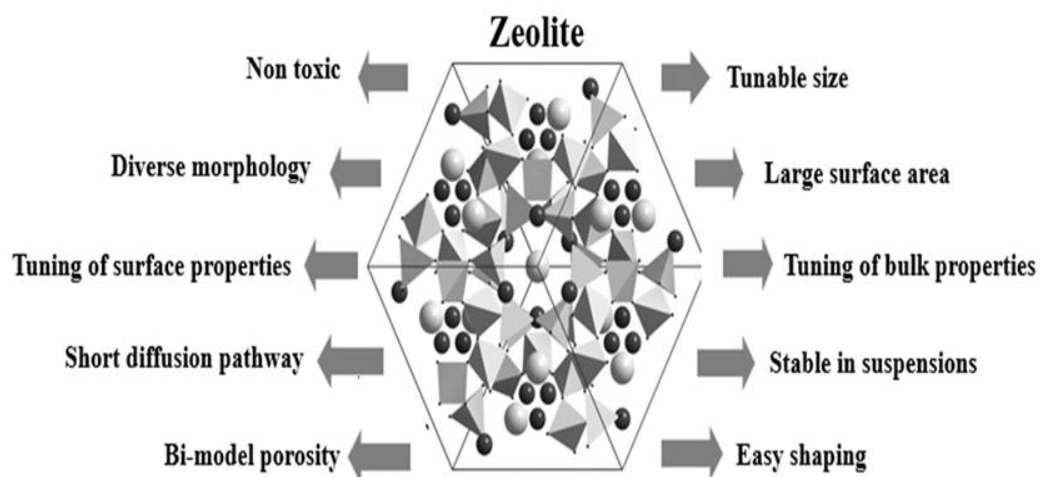


Figure 2.3. The properties of nanozeolites (Mintova, Grand & Valtchev, 2016).

2.6 Zeolite synthesis and formation

Essentially, different methods can be used to synthesize zeolites with various structures, properties and compositions. Zeolites can be formed naturally from volcanic ash where the synthetic zeolites are synthesized in the laboratory mimicking the natural process. This process is called hydrothermal process which was firstly used by Richard Barrer and Robert Milton in the 1940s for synthesizing zeolite A (Cundy and Cox, 2005). The hydrothermal process involves the chemical reaction of a reactive aluminosilicate precursor made up of water, mineralizer (e.g. NaOH, KOH or CsOH), alumina and silica sources at an elevated temperature (80-220 °C) under autogenous pressure and alkaline environments (Flanigen, Broach and Wilson, 2010) Alumina sources can be found in the formz of aluminum hydroxide, pure aluminum, aluminum isopropoxide and sodium aluminate. In addition, the sources of silica like silica sol, sodium silicate, amorphous silica and fumed silica are commonly used. The zeolites prepared are highly depending on the aluminum content used, because different types of zeolites exhibit different physical-chemical characteristics. In some cases, organic quaternary ammonium cation in the form of salt is added to the precursor hydrogel as

a template or as a structure-directing agent (SDA) to stabilize the framework structure of the zeolite system (Flanigen *et al.*, 2010). The resulting amorphous precursor containing silicate, aluminate, and organic template which is formed in a basic (high pH) medium, is typically heated to a temperature above 80 °C in a close system. For the crystallization below 100 °C, polypropylene bottle is used whereas stainless steel autoclave is used when the hydrothermal process is conducted at 100-250 °C. The reactants in the form of aluminosilicate polymer network remain amorphous before it experiences induction, nucleation and finally crystallization after a certain time. During crystallization, an equal mass of amorphous solid is transformed into crystalline zeolite phase. When the crystallization is complete, the solid product is separated from the mother liquors using filtration (for big crystals larger than 1 µm) or high-speed centrifugation (for small crystals smaller than 1 µm), washed with distilled water in order to obtain pure zeolite crystals (Cundy and Cox, 2005). The processes of synthesizing and preparation of zeolite solids are shown in Figure 2.4. In general, the chemical composition of the precursor hydrogel has little resemblance to that of the final zeolitic product. The properties of zeolite formed (e.g. crystalline phase, size, morphology and porosity) are determined by the nature of reactants (silica and alumina sources), chemical composition, pH of the precursor, temperature, pressure and

organic template used (Wernert *et al.*, 2005; Cejka, Corma and Zones, 2010). The functions of the reactants in the zeolite synthesis are summarized as in Table 2.1.

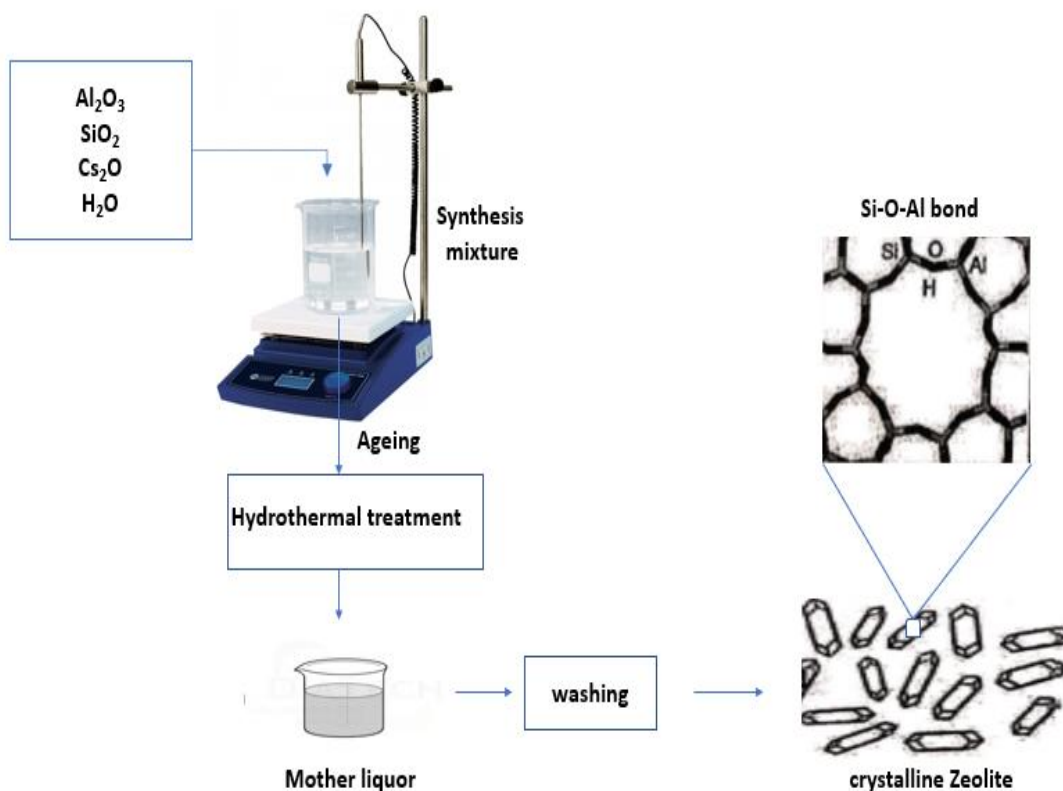


Figure 2.4. Hydrothermal synthesis and purification processes of zeolite.

Table 2.1

Chemical sources and their respective functions in zeolite synthesis (van Bekkum et al., 2001).

Sources	Functions
SiO ₂	Primary building units of the framework
Al ₂ O ₃	Origin of framework charge
OH ⁻ , F ⁻	Mineralizer, guest molecule
Alkali cation, template	Counter ion of framework charge, guest molecule
H ₂ O	Solvent, guest molecule

2.7 Cesium aluminosilicate zeolites

Cesium aluminosilicate zeolites are of great interest to zeolite scientists and industries because of their promising applications as hosts for immobilization of ^{137}Cs in radioactive waste management. Unfortunately, only a few papers reporting the synthesis of Cs based zeolites are published (Ito, 1976; Bell *et al.*, 2008; Ghrear, 2019). In 1976, a new anhydrous cesium aluminosilicate with an ideal formula of $\text{CsAlSi}_5\text{O}_{12}$ was successfully synthesized by slow cooling the transparent amorphous cesium aluminosilicate melt (750–1420 °C) which contained a large amount of Ba-vanadate flux (Ito, 1976). The synthesized Cs-zeolite had 5-membered rings which were built by the Al and Si tetrahedra units and the crystal showed an orthorhombic structure. Later, another method to synthesize Cs-zeolite using the atomic pair distribution function (PDF) method was also reported (Bell *et al.*, 2008). In this method, the Cs-geopolymer ($\text{Cs}_2\text{O} \cdot \text{Al}_2\text{O}_3 \cdot 4\text{SiO}_2 \cdot 11\text{H}_2\text{O}$) was heated until it reached 1100 °C for 24 h. The resulting product was crystalline pollucite ($\text{CsAlSi}_2\text{O}_6$) which had a cubic structure. In 1953, the synthesis of pure cesium pollucite had been improved where it was crystallized under hydrothermal condition at lower temperature (450 °C) using cesium aluminosilicate gel (Barrer and McCallum, 1953).

Cs-pollucite is a zeolite mineral which belongs to the analcime zeolite family (Yokomori, Idaka, 1998; Taylor, 1972; Beger, 1969; Ogorodova *et al.*, 2003). Cs-pollucite is one of the best storage alternatives for radioactive Cs owing to its 6-membered ring of 2.8 Å that can prison the radioactive $^{137}\text{Cs}^+$ which has a size of 3.34 Å. The radioactive cation is removed from water stream by the mechanism that the Cs^+ will be trapped inside the structure of pollucite when pollucite framework is formed. As a result, this harmful cation cannot be released from the pollucite structure without breaking the whole framework (Komarneni, McCarthy, Gallagher, 1978; Yokomori *et*

al., 2014). The channel system in pollucite zeolite contains many Cs ions which accommodate over 40 wt% Cs in the structure. The presence of Cs⁺ cations in the framework of Pollucite facilitates this zeolite as a basic catalyst due to the high electropositive cation of Cs⁺. In the crystal structure of Cs-pollucite, the Cs⁺ cations are uniformly distributed on the framework structure of pollucite where the distance between two Cs⁺ ions in the micropore channel is about 5.92 Å (Kamiya, Nishi, & Yokomori, 2008; Palmer *et al.*, 1997). Unfortunately, pollucite is usually synthesized at very high temperature (>240 °C) under hydrothermal condition (Gallagher and McCarthy, 1982; Goto, Matsuzawa and Matsuda, 1981; Mimura and Kanno, 1985; Torres-Martinez *et al.*, 1984). For instance, pollucite is crystallized at 240 °C within 6 days using chabazite zeolite as initial source (Barrer, 1950). If phillipsite zeolite is used as initial inorganic source, the pollucite can be obtained at 300 °C within 13 hours (Komarneni, 1985).

2.8 Applications of zeolites

Zeolites have a wide range of applications. The use of zeolites is promising and applicable particularly in the industrial sector. They are suitable for gas purification and separation, catalysis (e.g. petrochemical cracking, isomerization), ion-exchange (purification, water softening), construction, etc. (Pfenniger, 1999).

2.8.1 Zeolites in adsorption and separation

Zeolites are microporous materials which have uniform pores. Zeolites can be used in gas adsorption because of their shape selectivity property. This ability is based on the fact that they adsorb specific molecules which are smaller than their micropores

while rejecting larger molecules from entering into their micropores, resulting in selective adsorption and separation (Pfenniger, 1999). In this application, the micropores control the diffusion of guest molecules in zeolites based on the size, polarity and shape of the molecules. For example, when para-, meta- and ortho-xylene are filtered with silicalit-1 zeolite, only para-xylene is allowed to diffuse into the pores of zeolite while the other two isomers are forbidden (Pfenniger, 1999). Zeolites are mainly used for purification and deodorization of natural gasses through the removal of impurities including oil, carbon and sulfur dioxide (Auerbach, Carrado and Dutta, 2003) In addition, cation-containing zeolites are commonly used as dehumidifier due to their high-water affinity thanks to the electrostatic interaction of the metal cations.

2.8.2 Zeolites in ion exchange

Zeolite can be functioned as solid electrolytes. The charge-balance cations located on the surface of zeolites can easily be replaced by other ions, as they are freely mobile and not belong to the part of the zeolite framework (Pfenniger, 1999). When the zeolites are contacted with the solutions containing metal cations, ion exchange process between the metal cations with the non-framework metal cations will occur due to the electrostatic interaction (Kitsopoulos, 1999). Zeolites can be used as water softener in the detergent industry where they are a very promising candidate in replacing the phosphate-based water softener that can induce eutrophication. During the water softening process, the metal cations in the water that cause water hardening, such as magnesium and calcium ions, are exchanged with the cations (e.g. Na^+) from the zeolite (Endres *et al.*, 2001). As a result, no solid precipitation is formed when the concentration of magnesium and calcium cations is low. In the detergent industry, zeolites such as clinoptilolite, A and X are often used (Dyer, 1988). In addition,